Burns & Trauma, 2025, **13**, tkae068
https://doi.org/10.1093/burnst/tkae068
Research Article

Receptor activity-modifying protein 1 regulates the differentiation of mouse skin fibroblasts by downregulating α-SMA expression via suppression of high mobility group AT-hook 1 to promote skin wound repair

Ru Song[1,2], Jiaxu Ma[1,2], Siyuan Yin[1,2], Zhenjie Wu[1,2], Chunyan Liu[1,2], Rui Sun[1,2], Guoqi Cao[1,2], Yongpan Lu[1,2], Jian Liu[1,2], Linqi Su[1,2], Yibing Wang[1,2,3,*]

[1]Department of Plastic Surgery, The First Affiliated Hospital of Shandong First Medical University & Shandong Provincial Qianfoshan Hospital, No. 16766, Jingshi Road, Lixia District, Jinan, Shandong 250014, P. R. China
[2]Jinan Clinical Research Center for Tissue Engineering Skin Regeneration and Wound Repair, The First Affiliated Hospital of Shandong First Medical University & Shandong Provincial Qianfoshan Hospital, No. 16766, Jingshi Road, Lixia District, Jinan, Shandong 250014, P. R. China
[3]Department of Plastic Surgery, Shandong Provincial Qianfoshan Hospital, Shandong University, No. 44, Wenhua Xilu, Lixia District, Jinan, Shandong 250012, P. R. China

*Corresponding author. E-mail: ybwang@sdfmu.edu.cn

Abstract

Background: Skin innervation is very important for normal wound healing, and receptor activity-modifying protein 1 (RAMP1) has been reported to modulate calcitonin gene-related peptide (CGRP) receptor function and thus be a potential treatment target. This study aimed to elucidate the intricate regulatory effect of RAMP1 on skin fibroblast function, thereby addressing the existing knowledge gap in this area.
Methods: Immunohistochemical staining and immunofluorescence (IF) staining were used to measure the dynamic changes in the expression of RAMP1 and α-smooth muscle actin (α-SMA) in skin wound tissue in mice. Mouse skin fibroblasts (MSFs) stably transfected with Tet-on-Flag-RAMP1 overexpression (OE) and Tet-on-Flag control (Ctrl) lentiviruses were constructed for *in vitro* experiments. High mobility group AT-hook 1 (HMGA1) plasmids and α-SMA plasmids were used to overexpress HMGA1 and α-SMA, respectively. An α-SMA siRNA was used to silence α-SMA. Quantitative real-time polymerase chain reaction (qPCR), western blot and IF staining analyses were used to determine the mRNA and protein levels in the cells in different groups. A scratch wound healing assay was used to evaluate the cell migration ability of different groups. Cleavage under targets and release using nuclease (CUT & RUN) assays and dual-luciferase reporter assays were used to predict and verify the interaction between HMGA1 and the α-SMA promoter.
Results: RAMP1 and α-SMA protein expression levels in the dermis changed dynamically and were negatively correlated during dorsal skin wound healing in mice. RAMP1 OE *in vitro* inhibited the differentiation and promoted the migration of MSFs by decreasing α-SMA expression via the suppression of HMGA1, which was shown for the first time to bind to the α-SMA promoter and increase α-SMA transcription. RAMP1 OE also modulated extracellular matrix (ECM) synthesis and remodeling by promoting collagen III and MMP9 expression and decreasing collagen I, MMP2, and tissue inhibitor of metalloproteinases 1 expression.
Conclusions: Our findings suggest that RAMP1 OE decreases differentiation and promotes migration in MSFs by downregulating α-SMA expression via the suppression of HMGA1 and modulates ECM synthesis and remodeling, revealing a novel mechanism regulating α-SMA transcription, providing new insights into the RAMP1-mediated regulation of fibroblast function, and identifying effective nerve-related targets for skin wound repair.

Keywords: Fibroblast differentiation; High mobility group AT-hook 1; Myofibroblast; Receptor activity-modifying protein 1; Skin wound healing; α-smooth muscle actin

Highlights

- This study is the first to show that the overexpression of RAMP1 can decrease fibroblast differentiation and promote the migration of mouse skin fibroblasts by inhibiting α-smooth muscle actin expression via the downregulation of HMGA1.
- HMGA1 was shown for the first time to be a transcription factor related to α-SMA in mouse skin fibroblasts.
- RAMP1 could also modulate the extracellular matrix synthesis and remodelling ability of mouse skin fibroblasts.

Background

During the skin wound healing process, different populations of dermal fibroblasts [1] are activated and differentiate into myofibroblasts, which are characterized by bundles of α-smooth muscle actin (α-SMA) [2,3] and function to regulate wound closure by promoting contraction [4], secreting signaling molecules [5,6] and synthesizing and remodeling the extracellular matrix (ECM) [7–9]. Davis et al. [10] reported that the expression of α-SMA in chronic wounds in diabetic patients was significantly lower than that in acute wounds in nondiabetic individuals, which led those authors to deduce that α-SMA-positive myofibroblasts were related to timely

Received: January 14, 2024. **Revised:** May 21, 2024. **Accepted:** October 11, 2024

wound healing. However, α-SMA has also been detected in many hypertrophic scars [11], and myofibroblasts are involved in many pathological scarring-related and fibrotic diseases [12], suggesting that excess myofibroblasts or abnormal myofibroblast persistence may contribute to pathological wound healing. A detailed elaboration of the dynamic regulation of α-SMA-positive myofibroblasts is necessary to understand wound healing and regulate the process effectively to achieve timely wound closure and high-quality healing [13].

Skin innervation plays important roles in wound healing, including the regulation of fibroblasts, but only a few high-quality studies on neuromediators and fibroblasts are available, and even those studies are somewhat outdated [12]. Our previous study revealed that p75 neurotrophin receptor (p75NTR) could regulate nerve growth factor (NGF)-induced myofibroblast differentiation by activating myocardin-related transcription factor A (MRTFA) [14]. Calcitonin gene-related peptide (CGRP) is a member of the neuroinflammatory factor family and is released when the skin is damaged [15]. CGRP has been reported to play an important role in wound healing [16–18]; however, a CGRP antibody used for migraine therapy led to impaired wound healing in one study [19], whereas J. Che´ret et al. [20] reported that CGRP could promote human dermal fibroblast adhesion and differentiation. However, those studies described only the phenomenon but not the involved mechanism. In addition, CGRP has side effects, such as pain [21], and a short half-life (10 min) in the plasma [22], which restrict its topical and systemic use.

Receptor activity-modifying protein 1 (RAMP1) is a CGRP receptor, along with calcitonin receptor-like receptor (CRLR) [23] and receptor component protein (RCP) [24–26]. RAMP1 is a single-pass transmembrane protein that is composed of 148 amino acids and has been reported to regulate CGRP function by influencing trafficking, conferring pharmacologic specificity to CRLR [27,28], and regulating cell proliferation [29] and differentiation [30]. RAMP1 was also reported to function independently of CRLR and CGRP, as it is expressed in the cortex and hippocampus, where overlap with CRLR does not occur [31–33]. RAMP1 is known to participate in wound healing by regulating angiogenesis and lymphangiogenesis [34], but the direct relationship between RAMP1 and fibroblasts has been poorly characterized. Our previous study revealed that RAMP1 can regulate the proliferation of mouse skin fibroblasts (MSFs) through the Gαi3/PKA/CREB/YAP axis, which is important for timely wound healing [35]. However, whether RAMP1 can also regulate the differentiation of MSFs and the details of the involved mechanism still require further investigation.

In this study, we found a negative correlation between the expression levels of RAMP1 and α-SMA in the dermis in mouse skin wounds. Through cellular and molecular experiments, we revealed that RAMP1 can regulate MSF differentiation and affect MSF mobility by regulating α-SMA transcription, thus affecting α-SMA protein levels via the regulation of transcription-related factor-high mobility group AT-hook 1 (HMGA1). We also showed that RAMP1 can regulate ECM synthesis and remodeling by regulating the expression of collagen I, collagen III, matrix metalloproteinase 2 (MMP2), MMP9, and tissue inhibitor of metalloproteinases 1 (TIMP1). Our study provides new evidence for the regulation of fibroblast function by RAMP1 and new insights into the molecular mechanisms of fibroblast differentiation, revealing potential nerve-related targets for wound healing.

Methods

Cell culture

MSFs were purchased from Guangzhou Jennio Biotech Company (Guangzhou, China). HEK293T cells were obtained from the CTCC (Meisen Chinese Tissue Culture Collections, Zhejiang, China). The MSFs and HEK293T cells were cultured in complete medium composed of DMEM (Gibco, USA) supplemented with 10% tetracycline-free fetal bovine serum (FBS) (Gibco) (v/v) and 1% antibiotics (BasalMedia, Shanghai, China) in a humidified incubator (Thermo Fisher Scientific, USA) at 37°C with 5% CO_2 and then seeded in plates (Corning, USA) and flasks (Thermo Fisher Scientific) for subsequent experiments.

Lentivirus and plasmid transfection

The Tet-on-Flag-RAMP1 overexpression (OE) and Tet-on-Flag control (Ctrl) lentiviruses were purchased from Genechem Company (Shanghai, China), and the primers used are listed in Table S1 (see online supplementary material). MSFs were seeded in 24-well plates at 30 000 cells per well and transfected with lentiviruses (MOI = 50) for 24 h, followed by incubation in fresh complete medium supplemented with puromycin (3 μg/ml; Beijing Solarbio & Technology Company, Beijing, China) for 48 h for the selection of stably transfected MSFs. These cells were further incubated for another 48 h with doxycycline (Dox, 5 μg/ml; MedChemExpress, USA) to confirm the transfection efficiency. Finally, MSFs stably transfected with the Tet-on-Flag-RAMP1 OE and Tet-on-Flag Ctrl lentiviruses were used for further experiments upon Dox induction.

The OE plasmids pcDNA3.1 HMGA1 (HMGA1), pcDNA3.1 α-SMA (α-SMA), and pcDNA3.1 empty vector (VEC), along with firefly luciferase reporter plasmids containing the α-SMA promoter region with wild-type (wt) and mutant (mt) HMGA1 binding sites (HBSs), and the Renilla luciferase plasmid were purchased from Syngentech Company (Beijing, China). The firefly luciferase reporter plasmid containing the α-SMA promoter region with mt HMGA1 binding site 1 (HBS1), the firefly luciferase reporter plasmid containing the α-SMA promoter region with mt HMGA1 binding site 2 (HBS2), and the firefly luciferase reporter plasmid containing the α-SMA promoter region with mt HMGA1 binding site 3 (HBS3) were constructed via chemical synthesis on the basis of the designed sequences, which are listed in Table S2 (see online supplementary material). Transfection was performed with PolyJet DNA In Vitro Transfection Reagent (SignaGen, USA) according to the manufacturer's protocol.

For siRNA transfection, 20 μM stock solutions of siRNA targeting α-SMA (si-α-SMA) and the negative Ctrl sequence (si-α-SMA NC) were prepared. The siRNA sequences were subsequently diluted and mixed at the following ratio: riboFECT™ CP Buffer (60 μl) plus siRNA stock solution (2.5 μl) and riboFECT™ CP reagent (6 μl). After the mixture was incubated for 15 min at room temperature to allow the formation of transfection complexes, each transfection complex was added to 931.5 μl of antibiotic-free complete medium. The cells were then treated with the transfection medium and incubated at 37°C with CO_2 for 24 h for subsequent experiments. The specific sequences used are listed in Table S3 (see online supplementary material).

Western blot analysis

Western blot analysis of protein expression was performed as described in previously published studies [14,36–38]. Total protein was labelled with No-Stain reagent (Thermo Fisher Scientific) according to the manufacturer's instructions and used as a loading control. The primary antibodies used in this study were as follows: anti-RAMP1, anti-MMP2 and anti-MMP9 (1:1000, rabbit, Abcam, UK); anti-α-SMA (1:1000, rabbit, Cell Signaling Technology (CST), USA); anti-collagen I and anti-collagen III (1:1000, rabbit, Proteintech, USA); and anti-TIMP1, anti-transforming growth factor β1 (TGFβ1), anti-TGFβ3, and anti-HMGA1 (1:1000, mouse, Santa Cruz Biotechnology, USA) antibodies. The secondary antibodies used were as follows: HRP-conjugated goat anti-rabbit antibodies and HRP-conjugated goat anti-mouse antibodies (1:5000, CST).

qPCR analysis

For the quantitative analysis of mRNA expression, RNA isolation, cDNA synthesis and quantitative real-time polymerase chain reaction (qPCR) were performed according to protocols published in our previous articles [14,36–38]. The mRNA levels were normalized to the expression level of β-actin in the matched samples. The primers used are listed in Table S4 (see online supplementary material).

Scratch wound healing assay

The migration of MSFs was measured via an *in vitro* monolayer scratch wound healing assay. The cells subjected to different treatments were seeded in 12-well plates (500 000 cells per well) with complete culture medium supplemented with Dox (5 μg/ml). After 12 h, when the cells reached confluence, the monolayer was scratched with a 10 μl pipette tip and washed with PBS (BasalMedia). The cells were subsequently cultured with low-serum (1% FBS) DMEM supplemented with Dox (5 μg/ml) for 24 h. Images of the wounds in each well were captured at 0, 12, and 24 h after scratching with an Olympus IX73 microscope (Olympus, Japan). The wound area was quantified with ImageJ software, and the cell migration rate was calculated and is presented as (wound area at 0 h—wound area of calculated time)/wound area at 0 h $\times$ 100%.

Immunofluorescence staining of cells

Immunofluorescence (IF) staining was performed as reported in our previous studies [14,36–38]. After being washed, fixed and permeabilized, the cells were incubated with anti-Flag (rabbit, 1:200, CST), anti-α-SMA (rabbit, 1:200, CST) and anti-F-actin (rat, 1:200, Abcam) primary antibodies at 4°C overnight and with goat anti-rabbit IgG H + L (Alexa Fluor 555), goat anti-rat IgG H + L (Alexa Fluor 555), goat anti-rabbit IgG H + L (Alexa Fluor 488), and goat anti-rat IgG H + L (Alexa Fluor 488) secondary antibodies (1:5000, CST) for 1 h at room temperature. Finally, the cells were stained with Hoechst (1:10 000; Invitrogen, USA) for 30 min at room temperature, followed by sealing with ProLong Gold Antifade Reagent (Invitrogen). Images were captured with a Nikon Eclipse Ti2 confocal laser scanning microscope (Nikon Instruments (Shanghai) Company, Shanghai, China).

Animals

Fifteen male C57BL/6 J mice (6 weeks old and 20 $\pm$ 2 g) were purchased from Beijing Vital River Laboratory Animal Technology Company (China). All the mice were housed in a 23 $\pm$ 2°C environment with a 12-h light/dark cycle. All the animal studies were approved by the Experimental Animal Ethics Committee of the First Affiliated Hospital of Shandong First Medical University (approval number: SYDWLS[2021]002) and were conducted in strict accordance with the U.K. Animals (Scientific Procedures) Act, 1986, and the Guide for the Care and Use of Laboratory Animals.

Wound experiments

After the mice were anaesthetized with 1% pentobarbital sodium (50 mg/kg, i.p.) and the dorsal hair was shaved, the skin was cleaned with 70% ethanol. The intersections—4 cm away from the base of the neck and 7 mm away from the midline—on either side of the dorsal midline were marked as center points for wound creation. A sterile biopsy tool with a diameter of 5 mm was subsequently used to make full-thickness skin wounds around the center point. The time at which the wound was created was defined as Day 0; the time point 24 h after surgery was defined as Day 1; and the time point 48 h after surgery was defined as Day 2, with the subsequent time points being defined in a similar manner. Each mouse was subsequently housed in a separate cage.

On Days 1, 3, 5, and 7, three randomly chosen mice were sacrificed with high-dose pentobarbital sodium for skin wound tissue collection. The wound area along with 3 mm of surrounding skin was excised after sacrifice, fixed in 10% formalin fixative and embedded in paraffin for subsequent sectioning and staining.

Immunohistochemical staining and IF staining of skin tissues

The fixed and embedded skin tissue was sliced into 3-μm-thick sections for immunohistochemical (IHC) staining and IF staining. After deparaffinization and rehydration, antigen retrieval was performed using a sodium citrate solution (Solarbio). For IHC staining, the sections were treated to block peroxidase activity with reagent #1 from the IHC kit (ZSGB-BIO, Beijing, China), blocked with reagent #2 (goat serum) for 1 h at room temperature and incubated with primary rabbit antibodies against RAMP1 (1:300; Abcam) and α-SMA (1:300; CST) at 4°C overnight. The sections were subsequently incubated with reagent #3 (the secondary antibody conjugated with biotin) for 15 min at room temperature, incubated with reagent #4 (HRP-labelled streptavidin working solution) for 15 min at room temperature and stained with DAB (ZSGB-BIO) before counterstaining with hematoxylin (Solarbio). After dehydration, clearing and sealing with resin, the tissue sections were imaged with an Olympus IX73 microscope. The integrated optical density (IOD)/area for the dermis was calculated with ImageJ software and recorded as the mean density. For IF staining, the sections were permeabilized, blocked, and subsequently incubated with an anti-RAMP1 antibody (rabbit, 1:200, Abcam) and an anti-α-SMA antibody (mouse, 1:200, CST) overnight at 4°C. After washing, the sections were incubated with a goat anti-rabbit IgG antibody (Alexa Fluor 555) and a goat anti-mouse IgG antibody (Alexa Fluor 488) for 1 h at room temperature. The sections were subsequently stained with Hoechst, followed by sealing with ProLong Gold Antifade Reagent. The images were captured with a Zeiss Celldiscoverer 7 with LSM900 multiplex airyscan confocal laser scanning fluorescence microscope (Zeiss, Oberkochen, Germany).

CUT&RUN assay

The cleavage under targets and release using nuclease (CUT&RUN) Assay Kit (CST) was used to probe protein–DNA interactions according to the manufacturer's instructions. Briefly, MSFs (100 000 cells) were washed with wash buffer, bound to concanavalin A beads, permeabilized with wash buffer containing digitonin and incubated with an anti-HMGA1 antibody (1:100, Santa Cruz Biotechnology), an anti-trimethylated histone H3 (Lys4) (H3K4me3) antibody or an IgG isotype Ctrl (CST) antibody overnight at 4°C with gentle rocking. Then, Protein A–Protein G–Micrococcal Nuclease was added to the cell–bead sample, which was subsequently incubated for 1 h at 4°C. Cleavage was performed by adding $CaCl_2$ and incubating the sample on ice for 30 min, and the digestion was stopped via the addition of one volume of stop buffer. The samples were subsequently incubated at 37°C for 30 min to digest the RNA and release DNA fragments and then centrifuged for 5 min at 16 000 × g at 4°C to recover the supernatant. The target DNA was subsequently extracted from the supernatant with DNA purification buffers and spin columns (CST) and quantified via qPCR and agarose gel electrophoresis. The primers used are listed in Table S5 (see online supplementary material).

Dual-luciferase reporter assay

HEK293T cells were seeded in 6-well plates and transfected with the HMGA1 plasmid, Renilla luciferase plasmid or firefly luciferase plasmid containing the specific wt or mt α-SMA promoter region for 24 h. After cell lysis, the luciferase activity was quantified with a dual-luciferase reporter kit (Beyotime) and an iMark Microplate Absorbance Reader (Bio-Rad Laboratories, USA). The relative luciferase activity was calculated by normalizing the firefly luciferase (Fluc) activity to the Renilla luciferase (Rluc) activity.

Quantitative proteomic analysis

MSFs stably transfected with the Tet-on-Flag-RAMP1 OE lentivirus or Tet-on-Flag Ctrl lentivirus and treated with Dox (5 μg/ml) for 48 h were harvested and stored at −80°C until the time of analysis. Tandem mass tag technology was used for quantitative proteomic analysis by Shanghai Applied Protein Technology (Shanghai, China). The normalized label-free quantification intensity on a log2 scale was used for differential expression analysis with a *t* test. Bioinformatics analysis was performed with R software v4.0.2 (R Foundation for Statistical Computing), and the screening criterion for differentially expressed proteins (DEPs) was a P value < 0.05.

Statistical analysis

The data, which were tested for normality and confirmed to be normally distributed, are presented as the means ± standard deviations (SDs) from three independent experiments and were analysed with GraphPad Prism 9 (USA). Student's *t* test was used for two-group comparisons, whereas one-way ANOVA was used for multiple group comparisons. Following one-way ANOVA, the Dunnett test was used as a post hoc test to compare the mean value of each column with the mean value of a control column, whereas the Bonferroni correction was used to compare the means of preselected pairs of columns. Two-way ANOVA was used to assess the influence of time and treatment factors on the data. Correlations between gene expression levels were analysed via Pearson's correlation analysis. P values<0.05 (*), P values<0.01 (**) and P values<0.001 (***) were considered to indicate statistical significance.

Results

RAMP1 and α-SMA protein levels change dynamically and are negatively correlated during the process of skin wound healing in mice

To investigate the roles and relationships of RAMP1 and α-SMA in wound healing, we conducted IHC and IF staining to assess their protein expression in the dermis in mouse skin wounds on Days 1, 3, 5, and 7 after wound induction. RAMP1 was expressed in both the epidermis and dermis in mouse skin wounds, whereas α-SMA was detected in the dermis and subcutaneous tissues (Figure 1a and b). Notably, α-SMA and RAMP1 were colocalized in the dermis. Our IHC staining analysis revealed a gradual increase in RAMP1 levels in the dermis from Days 1 to 3 to 5, followed by a slight decrease on Day 7. In contrast, α-SMA protein expression decreased from Day 1 to Day 3 and Day 5 but increased on Day 7 compared with Day 5 (Figure 1a–c), which aligns with findings reported by Hasan et al. [39]. Further analysis revealed a significant negative correlation between α-SMA protein expression and RAMP1 levels ($R = -0.9166$, $P < 0.01$) (Figure 1d). These results elucidate the dynamic regulation and negative correlation of RAMP1 and α-SMA protein levels in the dermis during the process of skin wound healing in mice.

RAMP1 OE modulates the synthesis and remodeling characteristics of MSFs

To explore the impact of RAMP1 on MSF function *in vitro*, we constructed MSFs that were stably transfected with Tet-on-Flag-RAMP1 OE (RAMP1 OE) or Tet-on-Flag Ctrl (RAMP1 Ctrl) lentiviruses. Western blot, qPCR, and IF assays were conducted to validate the successful OE of Flag-RAMP1 (Figure 2a–d). We subsequently assessed how RAMP1 influences ECM production and remodeling, as these processes are considered crucial functions of myofibroblasts [2], and we found that RAMP1 OE promoted collagen III expression while inhibiting collagen I expression. Additionally, MSFs in the RAMP1 OE group presented elevated levels of MMP9 mRNA and protein and reduced levels of MMP2 and TIMP1 mRNA and protein compared with those in the RAMP1 Ctrl group (Figure 2e–g). Interestingly, RAMP1 OE also altered the secretion profile of fibroblasts, resulting in an increase in TGFβ1 levels and a decrease in TGFβ3 expression after RAMP1 OE (Figure 2e–g). These findings suggest that RAMP1 OE regulates the expression profile of proteins related to ECM homeostasis in MSFs.

RAMP1 OE suppresses α-SMA expression and promotes MSF migration

To further investigate the impact of RAMP1 on MSF differentiation in greater detail, we performed western blot and qPCR analyses to examine the expression of α-SMA, one of the most important hallmarks of fibroblast differentiation [2,3]. The data presented in Figure 3a–c demonstrate that the OE of RAMP1 led to a reduction in α-SMA expression at both the protein and mRNA levels, indicating a potential role of RAMP1 in regulating α-SMA expression at the

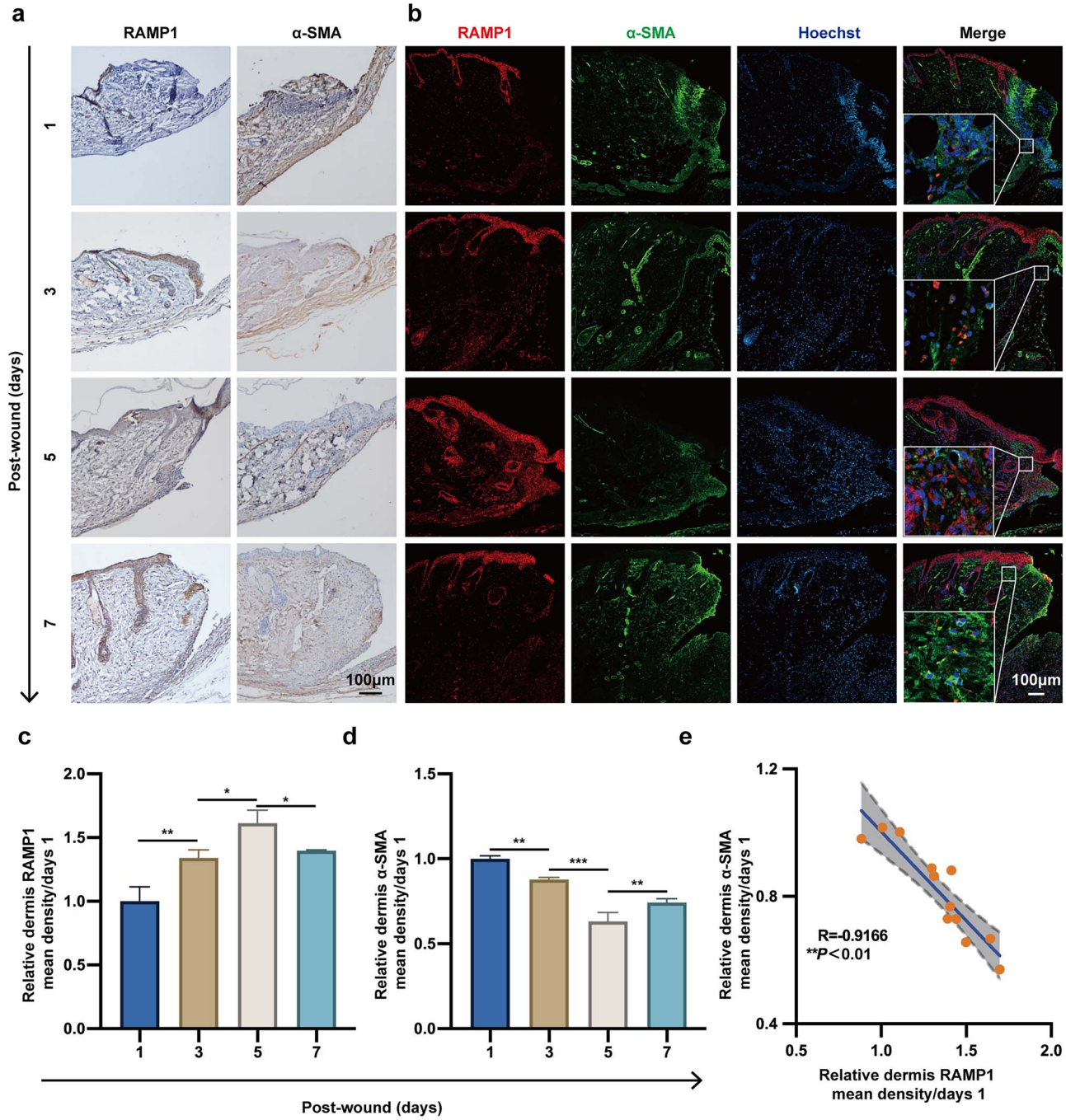

Figure 1. The protein expression levels of RAMP1 and α-SMA were negatively correlated in skin wound tissue in mice. (**a**) IHC staining for RAMP1 and α-SMA in acute wound tissues in mice (10x, scale bars: 100 μm). (**b**) Confocal images of IF staining for RAMP1, α-SMA, and Hoechst in acute wound tissues in mice (scale bars: 100 μm). (**c**) Quantification of the relative expression of RAMP1 in the dermis shown in a. (**d**) Quantification of the relative expression of α-SMA in the dermis shown in a. (**e**) Pearson's correlation analysis of the relative expression levels of RAMP1 and α-SMA in the dermis shown in a. the data are presented as the means ± SDs of three independent experiments ($^{*}P < 0.05$, $^{**}P < 0.01$, and $^{***}P < 0.001$). *RAMP1* receptor activity-modifying protein 1, *IHC* immunochemistry, *IF* immunofluorescence, *SD* standard deviation

transcriptional level. Additionally, IF staining also revealed a decrease in α-SMA levels upon RAMP1 OE (Figure 3d). Given the controversial role of α-SMA expression in fibroblast migration after differentiation into myofibroblasts [40], we conducted scratch wound healing assays to evaluate fibroblast migration in the different experimental groups. Interestingly, our findings revealed a significant increase in the migration capacity of MSFs upon RAMP1 OE compared with that of the RAMP1 Ctrl group at both 12 and 24 h postscratching (Figure 3e and f).

To confirm that RAMP1 OE facilitates MSF migration by impeding MSF differentiation, we overexpressed α-SMA in RAMP1 OE MSFs and RAMP1 Ctrl MSFs (Figure 4a–c). Subsequent scratch wound assays indicated that α-SMA OE in these MSFs counteracted cell migration (Figure 4d and e). In conclusion, these results suggest that RAMP1 impedes

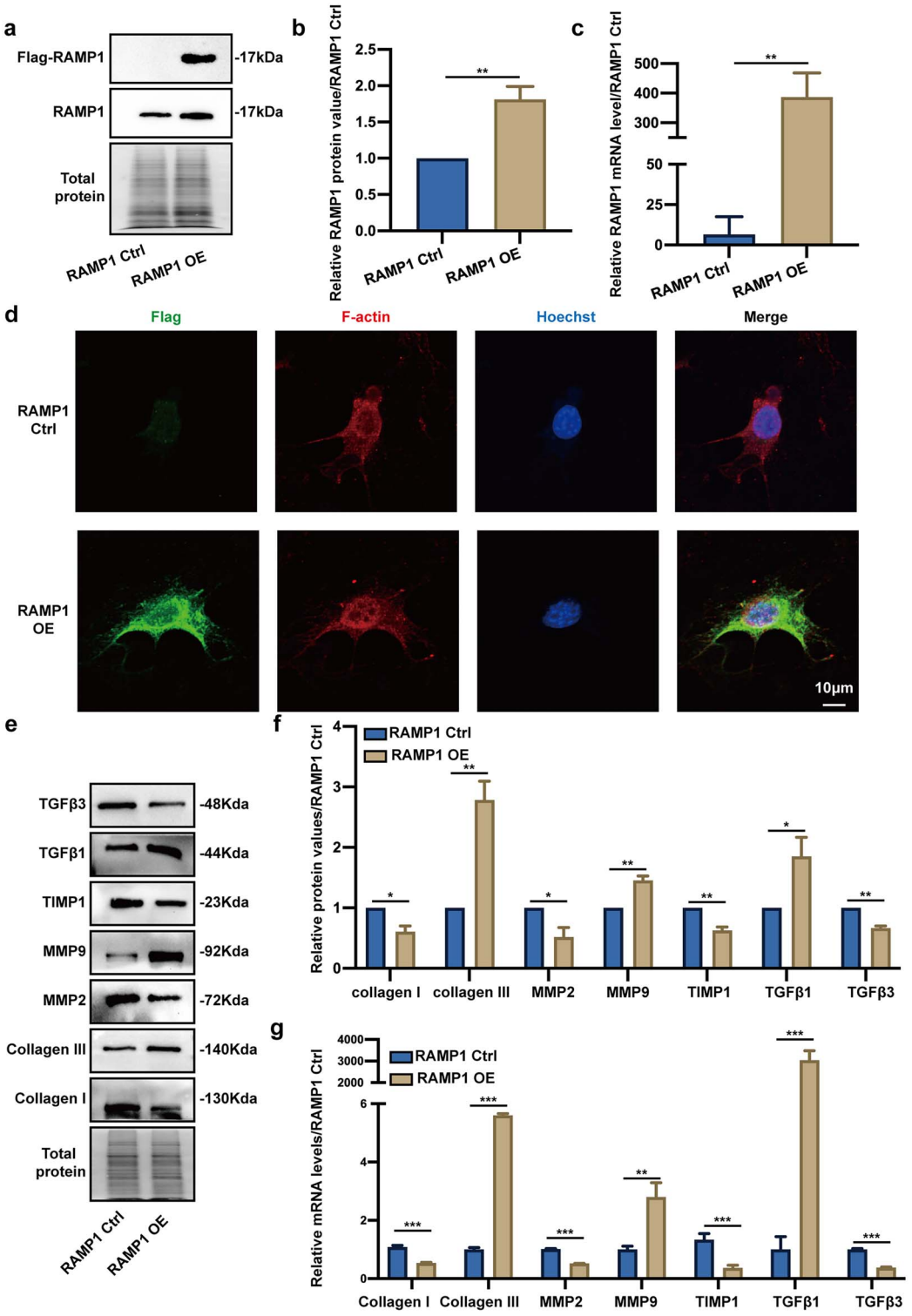

Figure 2. RAMP1 OE regulated collagen and MMP expression in MSFs. (**a**) Western blot of Flag-RAMP1 and RAMP1 in MSFs stably transfected with Tet-on-Flag-RAMP1 OE (RAMP1 OE) or Tet-on-Flag Ctrl (RAMP1 Ctrl) lentiviruses, followed by culture in medium supplemented with dox (5 μg/ml) for 48 h. Total protein was used as a loading control. (**b**) Quantification of the relative expression of RAMP1 in a. (**c**) qPCR analysis of RAMP1 mRNA levels in RAMP1 OE MSFs and RAMP1 Ctrl MSFs after culture in medium supplemented with dox (5 μg/ml) for 48 h. (**d**) Confocal images of IF staining for Flag, F-actin and Hoechst in RAMP1 OE MSFs and RAMP1 Ctrl MSFs obtained after culture in medium supplemented with dox (5 μg/ml) for 48 h (scale bar: 10 μm). (**e**) Western blot of collagen I, collagen III, MMP2, MMP9, TIMP1, TGFβ1, and TGFβ3 in RAMP1 OE MSFs and RAMP1 Ctrl MSFs obtained after culture in medium supplemented with dox (5 μg/ml) for 48 h. Total protein was used as a loading control. (**f**) Quantification of the relative expression levels of proteins in e. (**g**) qPCR analysis of collagen I, collagen III, MMP2, MMP9, TIMP1, TGFβ1, and TGFβ3 mRNA levels in RAMP1 OE MSFs and RAMP1 Ctrl MSFs after culture in medium supplemented with dox (5 μg/ml) for 48 h. The data are presented as the means ± SDs of three independent experiments (*$P < 0.05$, **$P < 0.01$, and ***$P < 0.001$). *RAMP1* receptor activity-modifying protein 1, *OE* overexpression, *Ctrl* control, *MMP* matrix metalloproteinase, *TIMP1* tissue inhibitor of metalloproteinases 1, *TGFβ* transforming growth factor β, *MSF* mouse skin fibroblast, *dox* doxycycline, *qPCR* quantitative real-time polymerase chain reaction, *IF* immunofluorescence, *SD* standard deviation

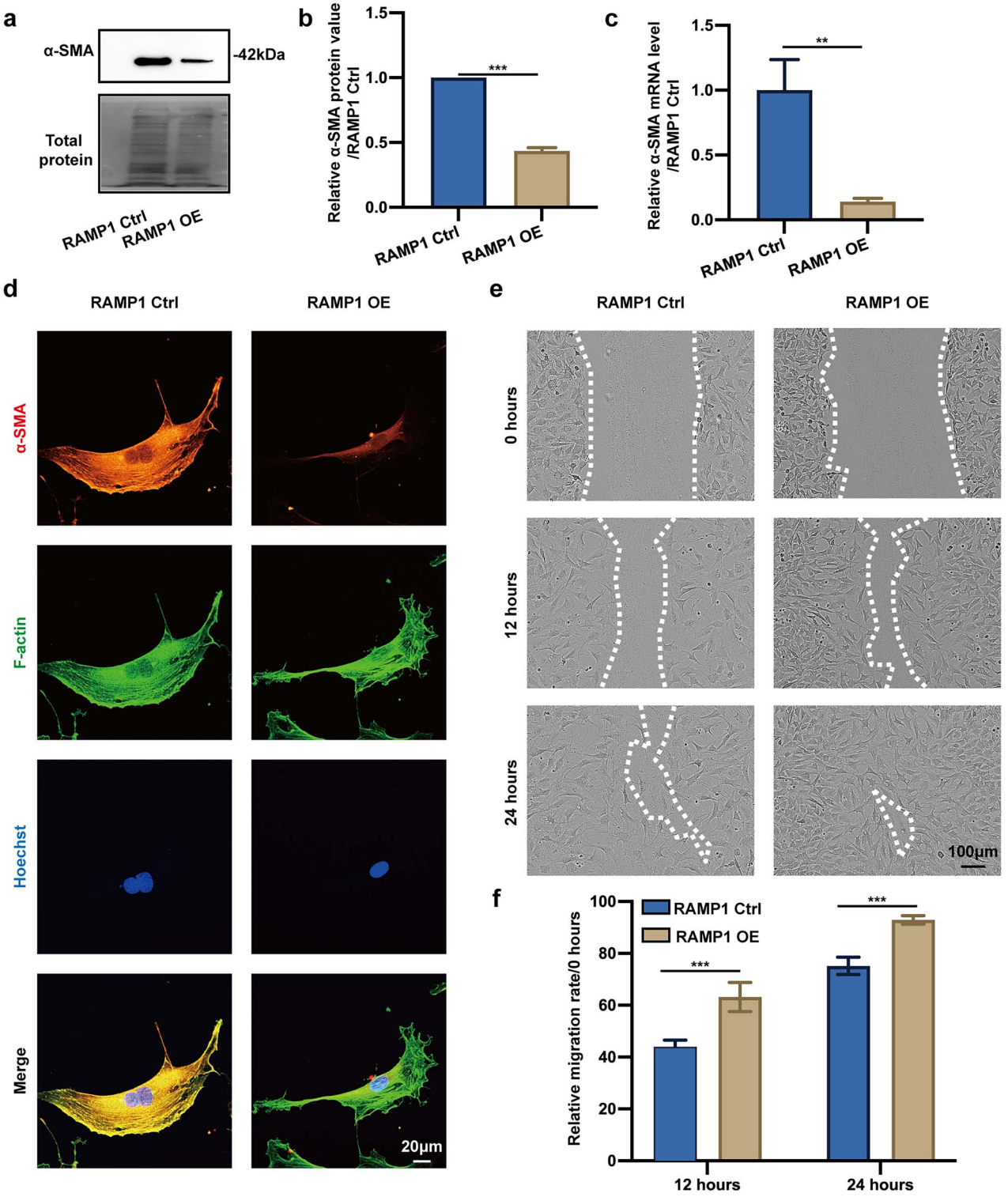

Figure 3. RAMP1 OE decreased α-SMA expression and promoted MSF migration. (**a**) Western blot of α-SMA in MSFs stably transfected with Tet-on-Flag-RAMP1 OE or Tet-on-Flag Ctrl lentiviruses, followed by culture in medium supplemented with dox (5 μg/ml) for 48 h. Total protein was used as a loading control. (**b**) Quantification of the relative expression levels of α-SMA in a. (**c**) qPCR analysis of α-SMA mRNA levels in RAMP1 OE MSFs and RAMP1 Ctrl MSFs after culture in medium supplemented with dox (5 μg/ml) for 48 h. (**d**) Confocal microscopy images of IF staining for α-SMA, F-actin and Hoechst in RAMP1 OE MSFs and RAMP1 Ctrl MSFs obtained after culture in medium supplemented with dox (5 μg/ml) for 48 h (scale bar: 20 μm). (**e**) Scratch wound healing assay showing the migration of RAMP1 OE MSFs and RAMP1 Ctrl MSFs at 0, 12, and 24 h after scratching (scale bar: 100 μm). (**f**) Quantification of the relative migration rate of MSFs in e. The data are presented as the means ± SDs of three independent experiments (** $P < 0.01$, and *** $P < 0.001$). *RAMP1* receptor activity-modifying protein 1, *OE* overexpression, *Ctrl* control, *α-SMA* α-smooth muscle actin, *MSF* mouse skin fibroblast, *dox* doxycycline, *qPCR* quantitative real-time polymerase chain reaction, *IF* immunofluorescence, *SD* standard deviation

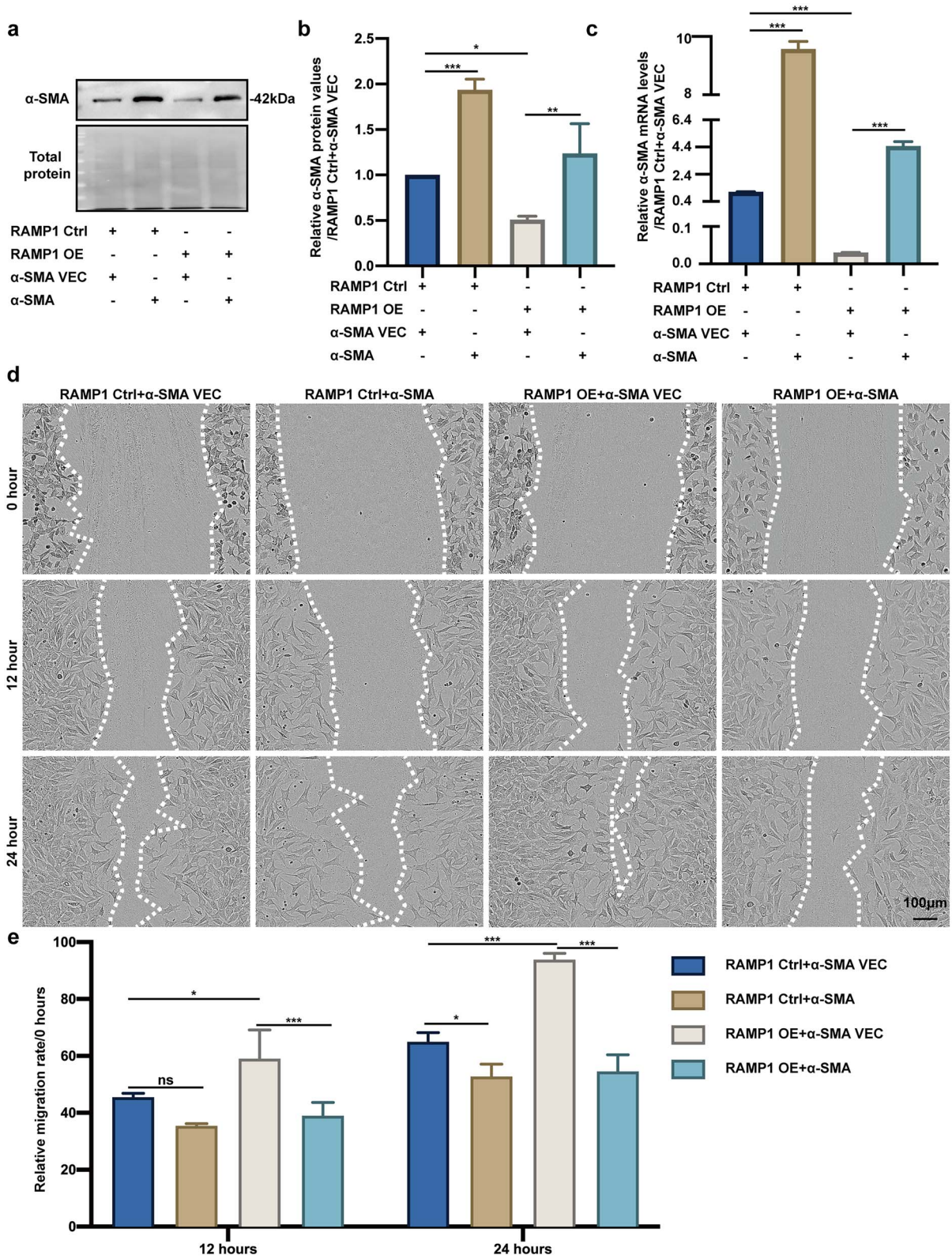

Figure 4. RAMP1 regulated the migration of MSFs via α-SMA. (**a**) Western blot of α-SMA in RAMP Ctrl+α-SMA VEC MSFs, RAMP Ctrl+α-SMA MSFs, RAMP OE + α-SMA VEC MSFs and RAMP1 OE + α-SMA MSFs. Total protein was used as a loading control. (**b**) Quantification of the relative expression levels of α-SMA in a. (**c**) qPCR analysis of the α-SMA mRNA levels in RAMP Ctrl+α-SMA VEC MSFs, RAMP Ctrl+α-SMA MSFs, RAMP OE + α-SMA VEC MSFs, and RAMP1 OE + α-SMA MSFs. (**d**) Scratch wound healing assay showing the migration of RAMP Ctrl+α-SMA VEC MSFs, RAMP Ctrl+α-SMA MSFs, RAMP OE + α-SMA VEC MSFs and RAMP1 OE + α-SMA MSFs at 0, 12, and 24 h after scratching (scale bar: 100 μm). (**e**) Quantification of the relative migration rate of MSFs in d. The data are presented as the means ± SDs of three independent experiments (* $P < 0.05$, ** $P < 0.01$, *** $P < 0.001$, *ns* not significant). *RAMP1* receptor activity-modifying protein 1, *OE* overexpression, *Ctrl* control, *VEC* vector, *α-SMA* α-smooth muscle actin, *MSF* mouse skin fibroblast, *qPCR* quantitative real-time polymerase chain reaction, *SD* standard deviation

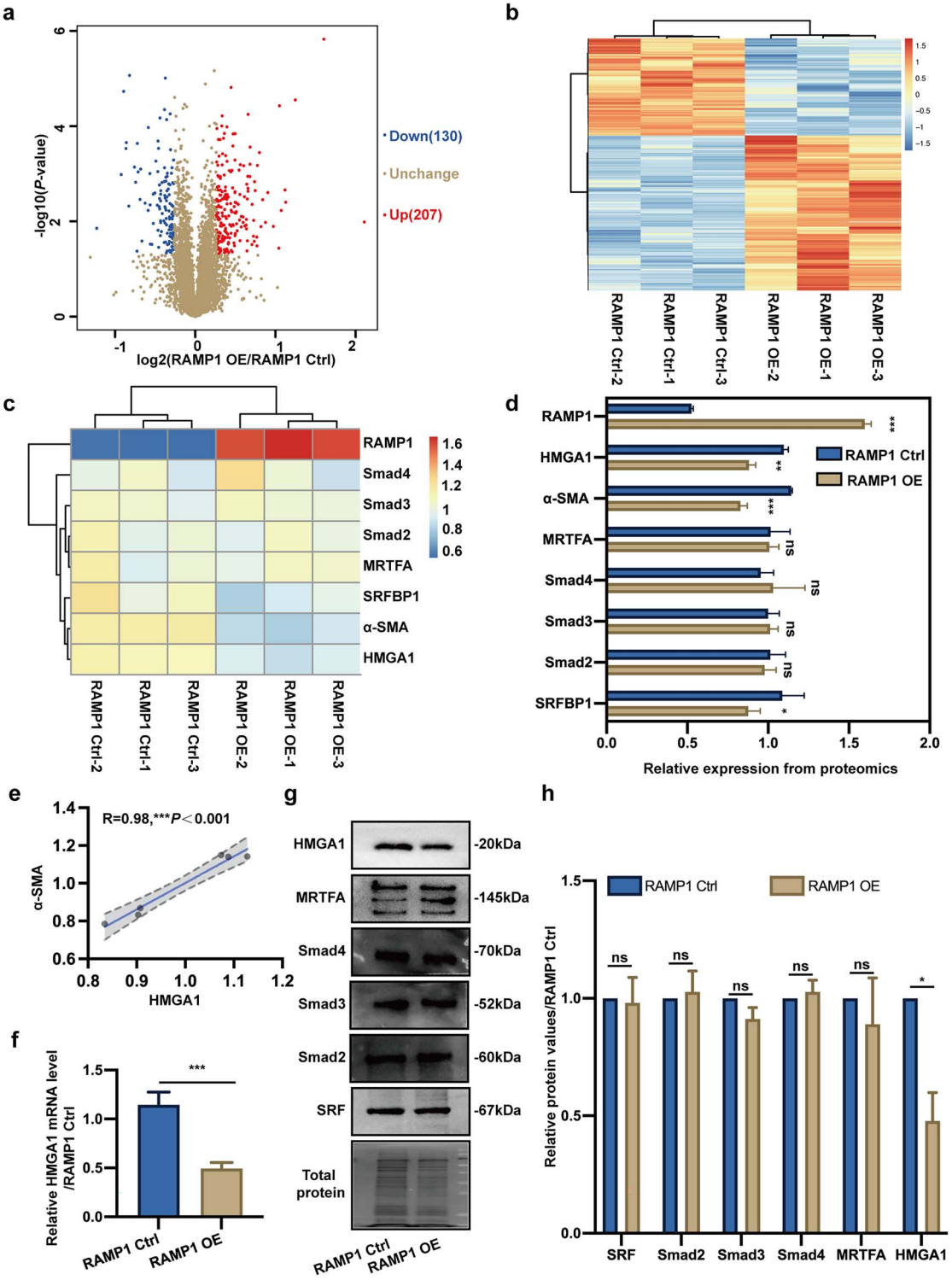

Figure 5. RAMP1 OE regulated the expression of HMGA1, which was associated with α-SMA transcriptional regulation in MSFs. (**a**) Volcano plot of the results from the proteomic analysis of MSFs stably transfected with Tet-on-Flag-RAMP1 OE or Tet-on-Flag Ctrl lentiviruses and subsequently cultured in medium supplemented with dox (5 μg/ml) for 48 h. (**b**) Heatmaps of the results from the proteomic analysis of DEPs in a. (**c**) Heatmap of selected DEPs, including Smad2, Smad3, Smad4, SRFBP1, MRTFA, HMGA1, α-SMA, and RAMP1 in a. (**d**) Relative expression of the selected DEPs in c. (**e**) Pearson's correlation analysis of the protein expression of α-SMA and HMGA1 in a. (**f**) qPCR analysis of HMGA1 mRNA levels in RAMP1 OE MSFs and RAMP1 Ctrl MSFs cultured in medium supplemented with dox (5 μg/ml) for 48 h. (**g**) Western blot of SRF, Smad2, Smad3, Smad4, MRTFA and HMGA1 levels in RAMP1 OE MSFs and RAMP1 Ctrl MSFs cultured in medium supplemented with dox (5 μg/ml) for 48 h. Total protein was used as a loading control. (**h**) Quantification of the relative expression levels of the proteins in g. The data are presented as the means ± SDs of three independent experiments (* $P < 0.05$, ** $P < 0.01$, and *** $P < 0.001$, *ns* not significant). *RAMP1* receptor activity-modifying protein 1, *OE* overexpression, *Ctrl* control, *MRTFA* myocardin-related transcription factor A, *SRFBP1* serum response factor-binding protein 1, *α-SMA* α-smooth muscle actin, *HMGA1* high mobility group AT-hook 1, *SRF* serum response factor, *MSF* mouse skin fibroblast, *dox* doxycycline, *qPCR* quantitative real-time polymerase chain reaction, *DEP* differentially expressed protein, *SD* standard deviation

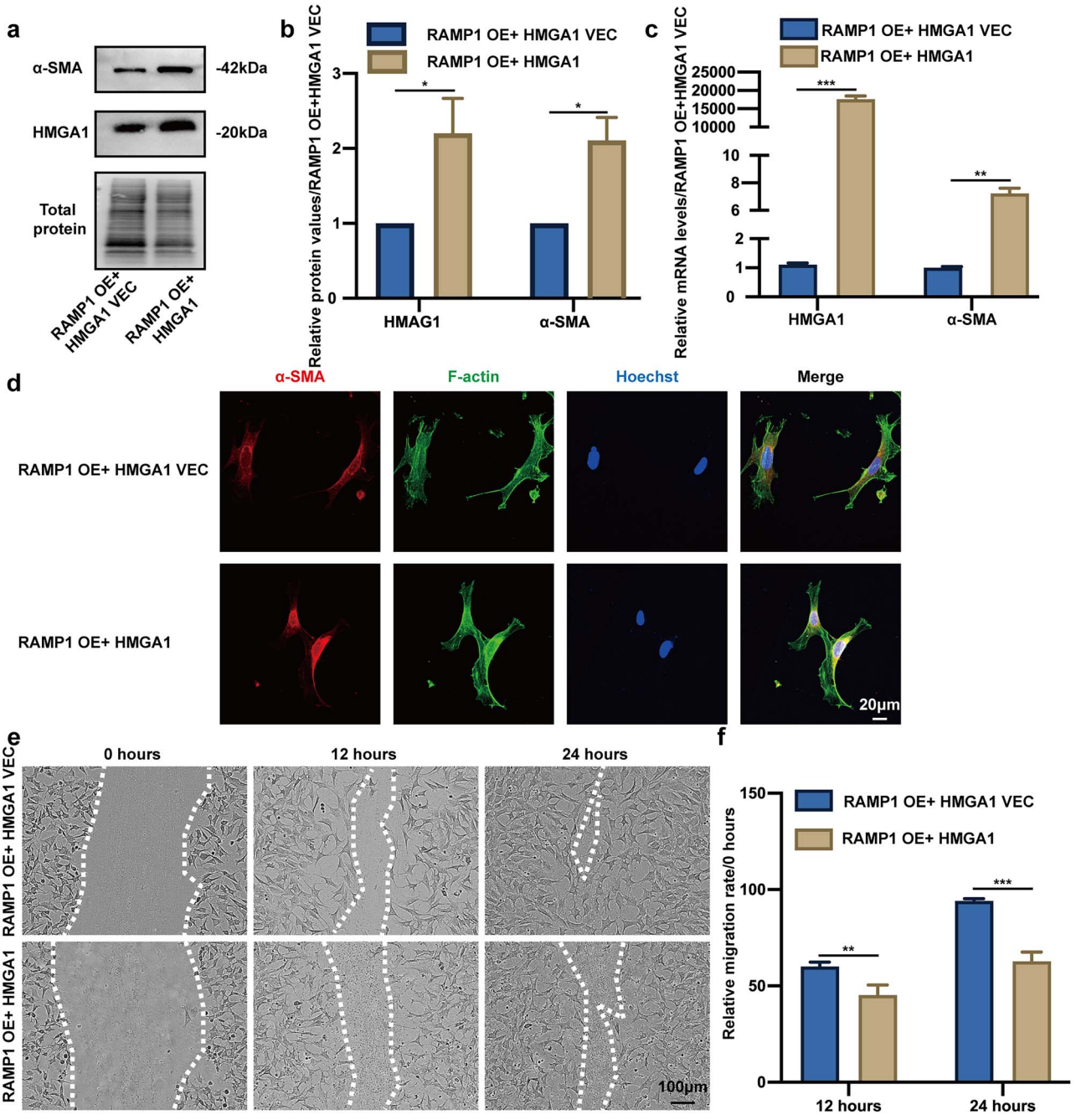

Figure 6. HMGA1 participated in the RAMP1-mediated regulation of α-SMA expression and MSF migration. (**a**) Western blot of HMGA1 and α-SMA in RAMP1 OE + HMGA1 VEC MSFs and RAMP1 OE + HMGA1 MSFs. Total protein was used as a loading control. (**b**) Quantification of the relative expression levels of HMGA1 and α-SMA in a. (**c**) qPCR analysis of HMGA1 and α-SMA mRNA levels in RAMP1 OE + HMGA1 VEC MSFs and RAMP1 OE + HMGA1 MSFs. (**d**) Confocal microscopy images of IF staining for α-SMA, F-actin and Hoechst in RAMP1 OE + HMGA1 VEC MSFs and RAMP1 OE + HMGA1 MSFs (scale bar: 20 μm). (**e**) Scratch wound healing assay showing the migration of RAMP1 OE + HMGA1 VEC MSFs and RAMP1 OE + HMGA1 MSFs at 0, 12, and 24 h after scratching (scale bar:100 μm). (**f**) Quantification of the relative migration rate of MSFs in e. The data are presented as the means ± SDs of three independent experiments (* $P < 0.05$, ** $P < 0.01$, and *** $P < 0.001$). *RAMP1* receptor activity-modifying protein 1, *OE* overexpression, *VEC* vector, *α-SMA* α-smooth muscle actin, *HMGA1* high mobility group AT-hook 1, *MSF* mouse skin fibroblast, *qPCR* quantitative real-time polymerase chain reaction, *dox* doxycycline, *SD* standard deviation

MSF differentiation while facilitating migration through the downregulation of α-SMA.

RAMP1 OE influences α-SMA transcription by inhibiting HMGA1 expression in MSFs

To elucidate the mechanisms by which RAMP1 regulates differentiation, we conducted a comprehensive quantitative proteomic analysis to compare protein levels between RAMP1 OE MSFs and RAMP1 Ctrl MSFs. The volcano plots and heatmaps shown in Figure 5a and b revealed 337 DEPs ($P < 0.05$), comprising 207 upregulated proteins (fold change >1.2) and 130 downregulated proteins (fold change <0.83). We subsequently scrutinized alterations in the protein expression of canonical and noncanonical factors associated

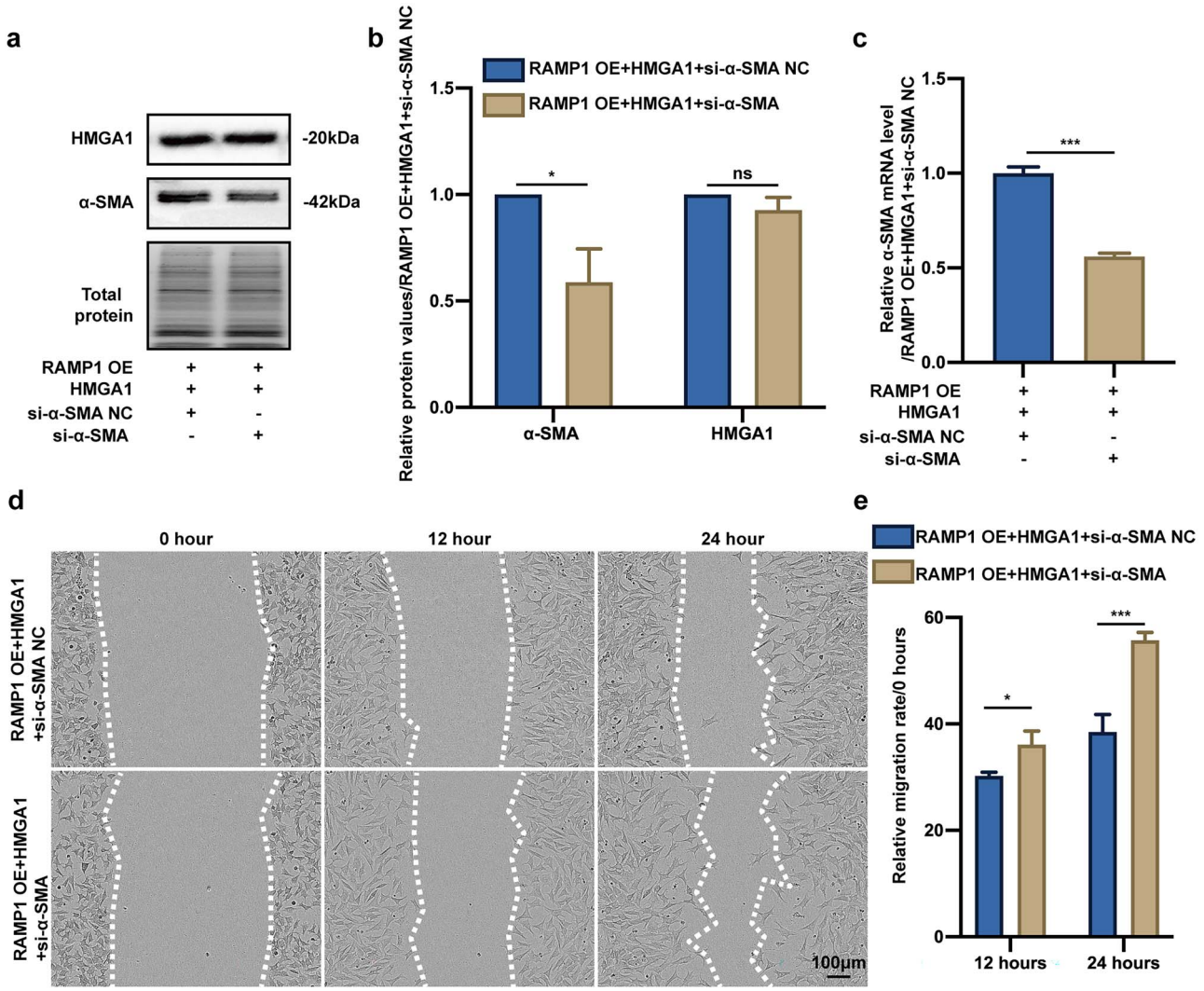

Figure 7. RAMP1 affects MSF migration by regulating α-SMA levels through HMGA1. (**a**) Western blot of HMGA1 and α-SMA in RAMP1 OE + HMGA1 + si-α-SMA NC MSFs and RAMP1 OE + HMGA1 + si-α-SMA MSFs. Total protein was used as a loading control. (**b**) Quantification of the relative expression levels of HMGA1 and α-SMA in a. (**c**) qPCR analysis of the α-SMA mRNA levels in RAMP1 OE + HMGA1 + si-α-SMA NC MSFs and RAMP1 OE + HMGA1 + si-α-SMA MSFs. (**d**) Scratch wound healing assay showing the migration of RAMP1 OE + HMGA1 + si-α-SMA NC MSFs and RAMP1 OE + HMGA1 + si-α-SMA MSFs at 0, 12, and 24 h after scratching (scale bar: 100 μm). (**e**) Quantification of the relative migration rate of MSFs in d. The data are presented as the means ± SDs of three independent experiments (* $P < 0.05$, *** $P < 0.001$, *ns* not significant). *RAMP1* receptor activity-modifying protein 1, *OE* overexpression, *NC* negative control, *HMGA1* high mobility group AT-hook 1, *α-SMA* α-smooth muscle actin, *MSF* mouse skin fibroblast, *qPCR* quantitative real-time polymerase chain reaction, *SD* standard deviation

with α-SMA transcription. The heatmap in Figure 5c and histogram in Figure 5d indicate that the expression levels of Smad2, Smad3, Smad4, serum response factor-binding protein 1 (SRFBP1) and MRTFA did not significantly change. As the OE of RAMP1 led to the downregulation of α-SMA expression, we searched for relevant transcription factors among the downregulated proteins. HMGA1 was identified as the most significantly differentially expressed transcription factor among the downregulated proteins in the proteomic analysis results. HMGA1 has also been reported to interact with serum response factor (SRF), leading to the upregulation of SM22α transcription [41]. Pearson's correlation analysis (Figure 5e) further confirmed a significant positive correlation between HMGA1 and α-SMA expression levels ($R = 0.98$, $P < 0.001$). Western blot analyses of α-SMA transcription-related proteins revealed that the OE of RAMP1 did not influence the expression levels of Smad2, Smad3, Smad4, MRTFA or SRF (Figure 5g and h). Furthermore, western blot and qPCR analyses confirmed that RAMP1 OE resulted in decreased expression of HMGA1 at both the protein and mRNA levels (Figure 5f–h). These findings suggest that HMGA1 could be a target for RAMP1-mediated regulation of α-SMA and differentiation.

HMGA1 OE upregulates α-SMA expression and inhibits MSF migration

To investigate the interplay between HMGA1 and RAMP1 in the regulation of α-SMA expression and differentiation, we initially transfected HMGA1 OE plasmids into RAMP1-overexpressing MSFs (RAMP1 OE + HMGA1). Western blot and qPCR analyses confirmed the successful OE of HMGA1 in the RAMP1 OE + HMGA1 group (Figure 6a–c). Subsequent analyses involving western blotting, qPCR, and IF staining revealed increases in both the expression and

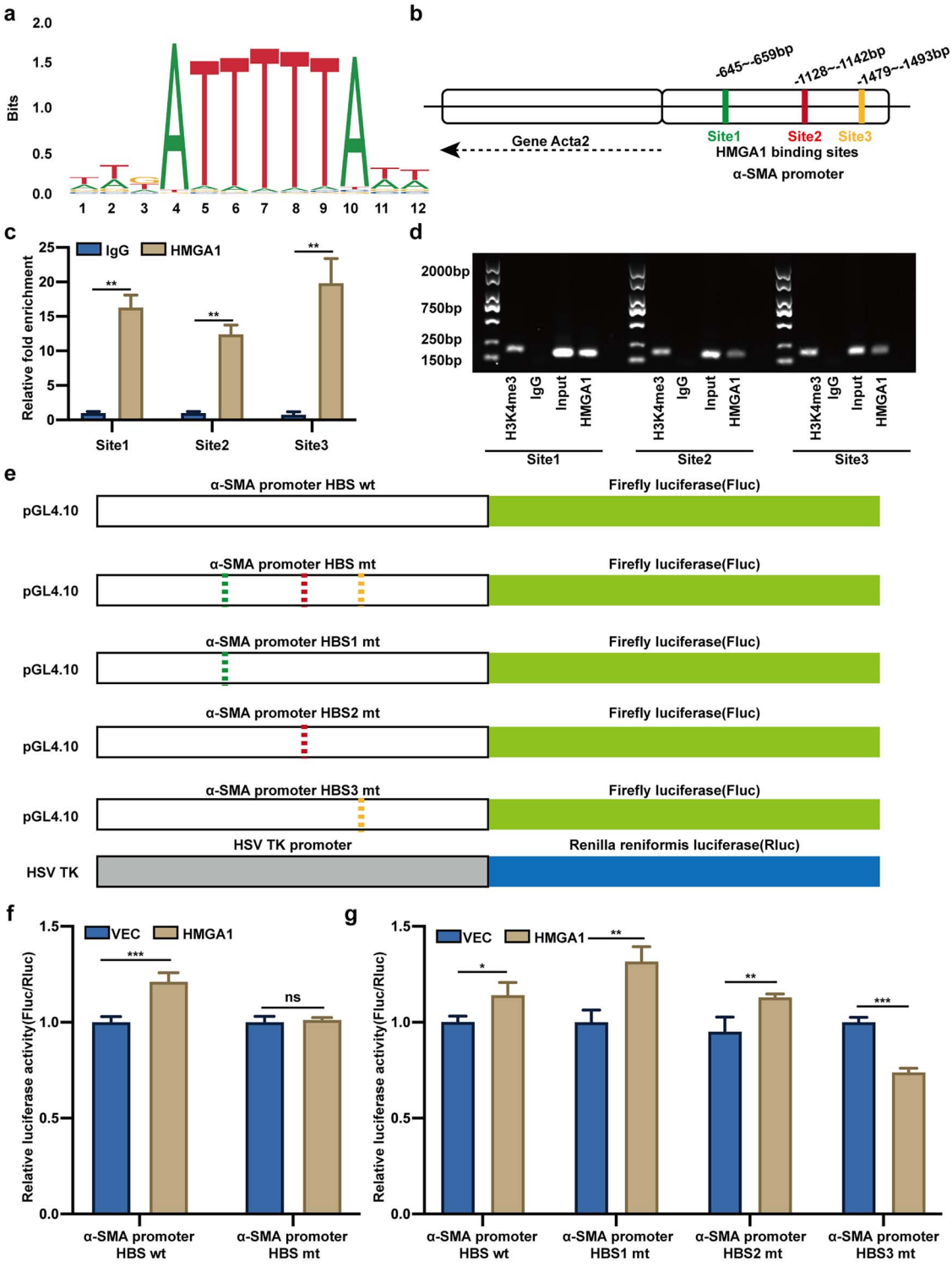

Figure 8. HMGA1 was newly identified as a transcription factor related to α-SMA. (**a**) The binding site sequence of HMGA1 was downloaded from the JASPAR promoter database. (**b**) Schematic diagram of the three predicted HBSs in the α-SMA promoter. (**c**) qPCR analysis of HMGA1 binding at the three predicted HBSs in the α-SMA promoter. (**d**) Agarose gel electrophoresis analysis of α-SMA promoter DNA amplified by qPCR with different primers. (**e**) Schematic diagrams of promoters fused to Fluc and Rluc. (**f**) Dual-luciferase reporter assay of HEK293T cells stably cotransfected with firefly reporter plasmids containing the α-SMA promoter with the wt HBSs or the α-SMA promoter with mt HBSs, pCDNA3.1 HMGA1 overexpression plasmids or pCDNA3.1 empty vector plasmids. Renilla luciferase reporter plasmids were included for normalization of the transfection efficiency data. (**g**) Dual-luciferase reporter assay of HEK293T cells stably cotransfected with firefly reporter plasmids containing the α-SMA promoter with wt HBSs, the α-SMA promoter with mt HBS1, the α-SMA promoter with mt HBS2 or the α-SMA promoter with mt HBS3, along with pCDNA3.1 HMGA1 overexpression plasmids or pCDNA3.1 empty vector plasmids. Renilla luciferase reporter plasmids were included for normalization of the transfection efficiency data. The data are presented as the means ± SDs of three independent experiments (* $P < 0.05$, ** $P < 0.01$, *** $P < 0.001$, *ns* not significant). *Acta2* alpha actin 2, *HMGA1* high mobility group AT-hook 1, *H3K4me3* trimethylated histone H3 (Lys4), *HBS* HMGA1 binding site, *Fluc* firefly luciferase, *Rluc* Renilla luciferase, *wt* wild-type, *mt* mutant, *VEC* vector, *qPCR* quantitative real-time polymerase chain reaction, *SD* standard deviation

transcription of α-SMA following HMGA1 OE (Figure 6–d). Furthermore, scratch wound healing experiments were conducted using RAMP1 OE + HMGA1 MSFs and RAMP1 OE + HMGA1 VEC MSFs to confirm whether HMGA1 regulation is also responsible for the promotion of migration. Surprisingly, migratory ability was reduced in the RAMP1 OE + HMGA1 MSF group (Figure 6e and f).

To determine whether HMGA1 inhibits cell migration through α-SMA, we silenced α-SMA with a small interfering RNA (si-α-SMA). Western blot and qPCR analyses demonstrated that si-α-SMA successfully reduced α-SMA expression in RAMP1 OE + HMGA1 cells (Figure 7a–c). Additionally, the scratch wound assay results revealed greater cell migration in the RAMP1 OE + HMGA1 + si-α-SMA group than in the RAMP1 OE + HMGA1 + si-α-SMA NC group (Figure 7d and e). These findings suggest that HMGA1 OE increases α-SMA expression while inhibiting cell migration, indicating that RAMP1 downregulates differentiation and promotes cell migration by suppressing HMGA1.

HMGA1 regulates α-SMA expression and differentiation at the transcriptional level

We then investigated the capacity of HMGA1, a chromatin structure modifier, to regulate α-SMA transcription, thereby influencing α-SMA expression and differentiation. Initially, by using the JASPAR promoter database, we identified the binding site sequence of HMGA1 (Figure 8a) and predicted three HBSs within the α-SMA promoter region at specific locations from the transcription start site (−645 to −659 bp: site 1; −1128 to −1142 bp: site 2; and − 1479 to −1493 bp: site 3) (Figure 8b; Table S6, see online supplementary material). A CUT&RUN assay was subsequently conducted to investigate potential protein–DNA interactions between HMGA1 and the transcriptional regulatory region of α-SMA. The CUT&RUN qPCR and DNA agarose gel electrophoresis results revealed that HMGA1 could bind to all three predicted binding sites in the α-SMA promoter region (Figure 8c and d). Next, a dual-luciferase reporter assay was used to determine the ability of HMGA1 to positively regulate α-SMA transcription. Reporter plasmids containing wt or mt HBSs in the α-SMA promoter were transfected into HEK293T cells. Notably, luciferase activity significantly increased with HMGA1 OE in the wt group but not in the mt group (Figure 8e and f), suggesting that HMGA1 may directly modulate α-SMA transcription by binding to at least one of the specific sites listed above. To pinpoint the specific targeted site, reporter plasmids containing mutated HBS1, HBS2, and HBS3 within the α-SMA promoter were cloned (Figure 8e). The results indicated that HBS1 and HBS2 did not affect HMGA1 transcriptional activity, whereas the HBS3-mt plasmid led to a notable reduction in HMGA1-mediated transcription, indicating that HBS3 is the probable transcription factor-binding site for HMGA1 (Figure 8g). Taken together, these results suggest that HMGA1 plays a crucial role in controlling α-SMA transcription and differentiation through this newly identified promoter site, establishing HMGA1 as a novel transcription factor related to α-SMA in MSFs.

Discussion

Neural factors, including neuropeptides such as CGRP, play important roles in the wound healing process [12,16,20]. Similarly, fibroblasts contribute significantly to wound repair through activities such as proliferation, differentiation, and protein synthesis and secretion [4,7–9]. However, the available research on the regulatory impact of CGRP on fibroblasts remains predominantly descriptive [20], and the underlying mechanism is still poorly understood. Furthermore, the direct application of neuropeptides either topically or systemically can lead to adverse effects [21]. RAMP1, a crucial component of the CGRP receptor [42], can not only modulate the pharmacological and signaling activity of the CGRP receptor but also function independently of CGRP [33], suggesting its potential as a target for drug development related to wound repair [42,43]. Consequently, investigating the regulatory role of RAMP1 in fibroblast function and the specific underlying mechanisms has significant value. In our current study, we initially observed a negative correlation between the expression levels of RAMP1 and α-SMA during the process of skin wound healing in mice. Our findings subsequently demonstrated that RAMP1 OE hindered differentiation and promoted cell migration by suppressing α-SMA transcription and protein expression through the downregulation of HMGA1 *in vitro*. Additionally, we noted that RAMP1 OE could impact the ECM synthesis and remodeling abilities of fibroblasts.

Fibroblasts have the capacity to secrete endogenous TGFβ1 [5], a powerful stimulator of fibroblast activation [44]. Interestingly, in culture plates, fibroblasts can form α-SMA stress fibers and undergo myofibroblast differentiation [40] without canonical induction by TGFβ1. In our study, we detected the baseline α-SMA level in the MSFs of the RAMP1 Ctrl group grown in culture plates under normal culture conditions without exogenous TGFβ1; thus, the relatively decreased levels of α-SMA protein and mRNA observed in the RAMP1 OE group confirmed that the OE of RAMP1 could decrease α-SMA expression.

α-SMA has been used as an indicator of myofibroblast differentiation in various studies [2,3,45]. Nevertheless, the specific effect of α-SMA on fibroblast behavior and function remains inadequately explored, with contradictory reports regarding its impact on fibroblast migration across different studies. While actin is conventionally recognized as a crucial motor protein for cell motility, the presence of α-SMA in fibroblasts has also been linked to increased motility. For example, an increase in α-SMA levels in human fetal lung fibroblasts has been shown to promote migration [46]. Conversely, α-SMA depletion in cardiac fibroblasts was not associated with a discernible effect on fibroblast migration [47]. The administration of AGEs can increase cardiac fibroblast migration by inducing their differentiation [48]. Nevertheless, α-SMA in fibroblasts can hinder motility, as evidenced by our experimental findings. Previous studies have also demonstrated that the presence of α-SMA impedes the migratory capabilities of human breast tissue-derived fibroblasts, with the inhibition of α-SMA synthesis significantly increasing fibroblast mobility [49]. Furthermore, the OE of α-SMA has been shown to retard the migration of human dermal fibroblasts [50].

The significant variations in the obtained results across different studies investigating the function of the α-SMA may stem from various factors. First, the use of cells from different organs cultured under varying conditions may have contributed to these discrepancies [46–50]. Fibroblasts sourced from distinct anatomical sites have distinct developmental

origins, and dermal and nondermal fibroblasts display discrepancies in gene expression profiles [1]. Therefore, alterations in α-SMA levels may yield varying effects on fibroblast behavior on the basis of the anatomical origin of the cells. Additionally, our study used mouse skin fibroblasts, and our findings align with prior research on skin dermal fibroblasts [49,50], suggesting that the inhibitory effect of α-SMA on fibroblast migration may be an intrinsic characteristic of skin fibroblasts. Drawing from the observed trend of RAMP1 expression during the wound healing process and our previous findings [35], we postulate that during the early stages of wound healing (from Day 1 to Day 5), a gradual increase in RAMP1 expression promotes MSF proliferation and migration to generate new granulation tissue, thereby facilitating rapid wound closure. In the later stage of wound healing (Day 7), the reduction in RAMP1 expression and increase in α-SMA expression slow migration, promote enhanced MSF differentiation and initiate contraction, contributing to high-quality wound healing. Further investigations are needed to elucidate the underlying mechanisms responsible for the α-SMA-mediated suppression of skin fibroblast migration.

The results from our *in vitro* experiments revealed that the OE of RAMP1 led to an increase in the expression of collagen III, MMP9 and TGFβ1 while concurrently downregulating TIMP1 expression. Notably, the fluctuations in the expression of these proteins increased during the early wound healing stage but decreased during the late stage, as previously reported [2,12,48–50], which coincided with the observed alterations in RAMP1 expression levels throughout the wound healing process. Consequently, we postulated that the dynamic variations in RAMP1 expression within wound tissue could contribute to the changes observed in collagen III, MMP9, and TGFβ1 expression during wound healing. Moreover, the suppression of collagen I, MMP2, and TGFβ3 induced by RAMP1 OE, coupled with decreased RAMP1 expression in the later stages of wound healing, might explain the reported increases in collagen I, MMP2, and TGFβ3 expression during the late phases of wound healing [12,51–53]. However, it is imperative to acknowledge that these deductions are solely based on logical interpretations derived from our *in vitro* cellular experiments and insights from *in vivo* experiments described in the literature. Given the complexity of the regulation of specific wound healing mechanisms, including collagen and MMP and TGFβ synthesis and metabolism, it is clear that such processes are intricately controlled by multiple factors and diverse cell populations [3,12,13]. Hence, the potential of RAMP1 to influence wound healing *in vivo* by modulating ECM synthesis and metabolism in fibroblasts requires further validation through rigorous *in vivo* experiments.

HMGA1, a nonhistone chromatin-binding protein, serves as a nuclear chromatin architectural factor [54], exerting control over gene transcription [55]. While HMGA1 is prominently expressed in embryonic cells, its levels remain relatively low in normal adult cells, suggesting that it plays a role in maintaining stemness and modulating cell differentiation [55,56]. Extensive research has linked HMGA1 to tumorigenesis, revealing its tumor-promoting abilities in small-cell lung cancer [57], breast cancer [58] and cervical cancer [59]. Moreover, its functions in pivotal processes within nontumor cells have also been highlighted. For example, studies by Egawa et al. [60] proposed that HMGA1 influences oligodendrocyte precursor cell differentiation by regulating merlin-related gene transcription. Similarly, Xie et al. [61] demonstrated that HMGA1 OE can activate fibroblasts by increasing FOXO1 transcription, thereby promoting cardiac fibrosis. Notably, our proteomic analyses revealed that HMGA1, rather than canonical α-SMA-related factors such as Smad2, Smad3, and Smad4 and noncanonical factors such as SRF and MRTFA [62], is a novel transcription factor for α-SMA in MSFs; this finding represents a significant contribution to the current understanding of this topic. Additionally, findings from Hopper et al. [63] support our observations, indicating that elevated HMGA1 levels can increase α-SMA and Slug expression in pulmonary arterial endothelial cells (PAECs), promoting their conversion to smooth muscle-like cells and potentially leading to pulmonary arterial hypertension. Furthermore, our study pinpointed site 3 as the probable binding site at which HMGA1 initiates α-SMA transcription. Despite previous reports that HMGA1 interacts with SRF to increase SM22α promoter activity [41], it remains essential to explore whether HMGA1-mediated α-SMA transcription is interconnected with SRF or other unidentified factors.

Moreover, the regulatory effects of a specific factor, such as RAMP1, on various downstream factors can have divergent mechanisms. Notably, our study revealed that the coordinated modulation of α-SMA and collagen I expression induced by RAMP1 OE correlated with the observations of McAndrews et al. [13], who reported significant reductions in collagen I expression and fiber abundance in nonhealing wounds of α-SMA-positive myofibroblasts conditional depletion mice. Interestingly, when we overexpressed the transcription factor HMGA1 in RAMP1 OE MSFs, we observed an increase in α-SMA expression without a corresponding increase in collagen I expression, contrary to our expectations (data not shown). This outcome implies that while HMGA1 influences the impact of RAMP1 on α-SMA expression, it does not exert a similar effect on collagen I mRNA synthesis.

Our study had several limitations. Although we identified a negative correlation between the expression levels of RAMP1 and α-SMA in the dermis during the wound healing process, it is important to note that this was only a general trend and was not solely due to the negative regulation of α-SMA by RAMP1 in fibroblasts. Although fibroblasts are crucial cells in wound healing [1,4,7–9] and colocalization of RAMP1 and α-SMA in the dermal layer was observed, other cells, such as endothelial cells and macrophages, also express RAMP1 and α-SMA during the wound healing process [9,35,63,64]. To investigate the impact of RAMP1 on fibroblast function *in vivo*, a transgenic mouse model in which RAMP1 is specifically expressed in fibroblasts is essential. Additionally, our experiments were limited to mouse skin fibroblasts, and it remains unclear whether the expression pattern of RAMP1 and its related regulatory mechanisms in human skin during wound healing parallel those observed in mice; thus, further verification is needed. Given the role of RAMP1 as a membrane receptor, future studies focusing on identifying specific agonists/antagonists of RAMP1 and evaluating their potential for promoting skin regeneration in animal models will be a key area of interest for our research in the future.

Conclusions

In summary, our study makes a novel contribution by demonstrating that RAMP1 OE suppresses HMGA1 expression,

consequently leading to reduced α-SMA expression. This signaling cascade promotes MSF migration through the inhibition of MSF differentiation. Notably, for the first time, we identified HMGA1 as a transcription factor that modulates α-SMA in MSFs. By revealing this intricate mechanism governing α-SMA transcription, our study offers new insights into the molecular processes underlying fibroblast differentiation. RAMP1 can also enhance ECM synthesis and remodeling. These findings elucidated the regulatory role of RAMP1 in the modulation of fibroblast behavior, potentially revealing new therapeutic targets for improving wound healing outcomes.

Abbreviations

RAMP1, receptor activity-modifying protein 1; CGRP, calcitonin gene-related peptide; IHC, immunochemistry; IF, immunofluorescence; α-SMA, α-smooth muscle actin; MSF, mouse skin fibroblast; OE, overexpression; Ctrl, control; HMGA1, high mobility group AT-hook 1; qPCR, quantitative real-time polymerase chain reaction; CUT&RUN, cleavage under targets and release using nuclease; ECM, extracellular matrix; p75NTR, p75 neurotrophin receptor; NGF, nerve growth factor; MRTFA, myocardin-related transcription factor A; CRLR, calcitonin receptor-like receptor; RCP, receptor component protein; MMP, matrix metalloproteinase; TIMP1, tissue inhibitor of metalloproteinases 1; FBS, fetal bovine serum; Dox, doxycycline; VEC, vector; wt, wild-type; HBS, HMGA1 binding site; mt, mutant; NC, negative control; TGFβ, transforming growth factor β; IOD, integrated optical density; H3K4me3: trimethylated histone H3 (Lys4); Fluc, firefly luciferase; Rluc, Renilla luciferase; DEP, differentially expressed protein; SD, standard deviation; SRFBP1, serum response factor-binding protein 1; SRF, serum response factor; PAECs, pulmonary arterial endothelial cells

Acknowledgements

We would like to thank the staff at the Center for Big Data Research in Health and Medicine, The First Affiliated Hospital of Shandong First Medical University & Shandong Provincial Qianfoshan Hospital, for their valuable contribution to this work.

Authors' contributions

Ru Song (Conceptualization [lead], Data curation [lead], Investigation [lead], Resources [lead]), Jiaxu Ma (Investigation [equal], Software [equal], Validation [equal]), Siyuan Yin (Formal Analysis [equal], Validation [equal], Visualization [equal]), Zhenjie Wu (Resources [equal], Supervision [equal]), Chunyan Liu (Investigation [equal], Resources [equal]), Rui Sun (Supervision [equal], Visualization [equal]), Guoqi Cao (Formal Analysis [equal], Validation [equal]), Yongpan Lu (Supervision [equal], Validation [equal]), Jian Liu (Validation [equal], Visualization [equal]), Linqi Su (Methodology [equal], Validation [equal]), Yibing Wang (Conceptualization [supporting], Funding Acquisition [lead]).

Supplementary data

Supplementary data are available at *Burns & Trauma Journal* online.

Ethical approval and consent to participate

Not applicable.

Consent for publication

Not applicable.

Conflicts of interest

The authors declare that they have no competing interests.

Funding

This study was supported by the National Natural Science Foundation of China (81972947 to YBW), the Natural Science Foundation of Shandong Province of China (Major Basic Research Program) (ZR2019ZD38 to YBW), the Key Research and Development Program of Shandong Province of China (No. 2019GSF108128 to YBW), the Academic Promotion Programme of Shandong First Medical University (2019LJ005 to YBW) and the Jinan Clinical Research Center for Tissue Engineering Skin Regeneration and Wound Repair.

Data availability

The datasets supporting the conclusions of this article are included within the article and its additional files.

References

1. Lynch MD, Watt FM. Fibroblast heterogeneity: implications for human disease. *J Clin Invest*. 2018;**128**:26–35. https://doi.org/10.1172/JCI93555.
2. Darby IA, Zakuan N, Billet F, Desmoulière A. The myofibroblast, a key cell in normal and pathological tissue repair. *Cell Mol Life Sci*. 2016;**73**:1145–57. https://doi.org/10.1007/s00018-015-2110-0.
3. Gurtner GC, Werner S, Barrandon Y, Longaker MT. Wound repair and regeneration. *Nature*. 2008;**453**:314–21. https://doi.org/10.1038/nature07039.
4. Grinnell F. Fibroblasts, myofibroblasts, and wound contraction. *J Cell Biol*. 1994;**124**:401–4. https://doi.org/10.1083/jcb.124.4.401.
5. Shu DY, Lovicu FJ. Myofibroblast transdifferentiation: the dark force in ocular wound healing and fibrosis. *Prog Retin Eye Res*. 2017;**60**:44–65. https://doi.org/10.1016/j.preteyeres.2017.08.001.
6. Zhou M, Zhao X, Liao L, Deng Y, Liu M, Wang J, *et al*. Forsythiaside a regulates activation of hepatic stellate cells by inhibiting NOX4-dependent ROS. *Oxidative Med Cell Longev*. 2022;**2022**:1–17. https://doi.org/10.1155/2022/9938392.
7. Mascharak S, Desjardins-Park HE, Davitt MF, Griffin M, Borrelli MR, Moore AL, *et al*. Preventing Engrailed-1 activation in fibroblasts yields wound regeneration without scarring. *Science*. 2021;**372**:eaba2374. https://doi.org/10.1126/science.aba2374.
8. Leavitt T, Hu MS, Borrelli MR, Januszyk M, Garcia JT, Ransom RC, *et al*. Prrx1 fibroblasts represent a pro-fibrotic lineage in the mouse ventral dermis. *Cell Rep*. 2020;**33**:108356. https://doi.org/10.1016/j.celrep.2020.108356.
9. Shook BA, Wasko RR, Rivera-Gonzalez GC, Salazar-Gatzimas E, López-Giráldez F, Dash BC, *et al*. Myofibroblast proliferation and heterogeneity are supported by macrophages during skin repair. *Science*. 2018;**362**:eaar2971. https://doi.org/10.1126/science.aar2971.
10. Davis FM, Tsoi LC, Wasikowski R, denDekker A, Joshi A, Wilke C, *et al*. Epigenetic regulation of the PGE2 pathway modulates macrophage phenotype in normal and pathologic wound repair. *JCI Insight*. 2020;**5**:e138443. https://doi.org/10.1172/jci.insight.138443.
11. Limandjaja GC, Belien JM, Scheper RJ, Niessen FB, Gibbs S. Hypertrophic and keloid scars fail to progress from the CD34(−)/α-smooth muscle actin (α-SMA)(+) immature scar phenotype and show gradient differences in α-SMA and p16 expression. *Br J Dermatol*. 2020;**182**:974–86. https://doi.org/10.1111/bjd.18219.
12. Lebonvallet N, Laverdet B, Misery L, Desmoulière A, Girard D. New insights into the roles of myofibroblasts and innervation during skin healing and innovative therapies to improve scar innervation. *Exp Dermatol*. 2018;**27**:950–8. https://doi.org/10.1111/exd.13681.

13. McAndrews KM, Miyake T, Ehsanipour EA, Kelly PJ, Becker LM, McGrail DJ, *et al.* Dermal αSMA(+) myofibroblasts orchestrate skin wound repair via β1 integrin and independent of type I collagen production. *EMBO J*. 2022;**41**:e109470. https://doi.org/10.15252/embj.2021109470.
14. Liu Z, Cao Y, Liu G, Yin S, Ma J, Liu J, *et al.* p75 neurotrophin receptor regulates NGF-induced myofibroblast differentiation and collagen synthesis through MRTF-A. *Exp Cell Res*. 2019undefined(undefined):111504;**383**:111504. https://doi.org/10.1016/j.yexcr.2019.111504.
15. Ellis A, Bennett DL. Neuroinflammation and the generation of neuropathic pain. *Br J Anaesth*. 2013;**111**:26–37. https://doi.org/10.1093/bja/aet128.
16. Granstein RD, Wagner JA, Stohl LL, Ding W. Calcitonin gene-related peptide: key regulator of cutaneous immunity. *Acta Physiol (Oxf)*. 2015;**213**:586–94. https://doi.org/10.1111/apha.12442.
17. Toda M, Suzuki T, Hosono K, Kurihara Y, Kurihara H, Hayashi I, *et al.* Roles of calcitonin gene-related peptide in facilitation of wound healing and angiogenesis. *Biomed Pharmacother*. 2008;**62**:352–9. https://doi.org/10.1016/j.biopha.2008.02.003.
18. Roggenkamp D, Köpnick S, Stäb F, Wenck H, Schmelz M, Neufang G. Epidermal nerve fibers modulate keratinocyte growth via neuropeptide signaling in an innervated skin model. *J Invest Dermatol*. 2013;**133**:1620–8. https://doi.org/10.1038/jid.2012.464.
19. Wurthmann S, Nägel S, Hadaschik E, Schlott S, Scheffler A, Kleinschnitz C, *et al.* Impaired wound healing in a migraine patient as a possible side effect of calcitonin gene-related peptide receptor antibody treatment: a case report. *Cephalalgia*. 2020;**40**:1255–60. https://doi.org/10.1177/0333102420933571.
20. Chéret J, Lebonvallet N, Buhé V, Carre JL, Misery L, Le Gall-Ianotto C. Influence of sensory neuropeptides on human cutaneous wound healing process. *J Dermatol Sci*. 2014;**74**:193–203. https://doi.org/10.1016/j.jdermsci.2014.02.001.
21. Holzer P. Neurogenic vasodilatation and plasma leakage in the skin. *Gen Pharmacol*. 1998;**30**:5–11. https://doi.org/10.1016/S0306-3623(97)00078-5.
22. Russell FA, King R, Smillie SJ, Kodji X, Brain SD. Calcitonin gene-related peptide: physiology and pathophysiology. *Physiol Rev*. 2014;**94**:1099–142. https://doi.org/10.1152/physrev.00034.2013.
23. Hinson JP, Kapas S, Smith DM. Adrenomedullin, a multifunctional regulatory peptide. *Endocr Rev*. 2000;**21**:138–67.
24. Dickerson IM. Role of CGRP-receptor component protein (RCP) in CLR/RAMP function. *Curr Protein Pept Sci*. 2013;**14**:407–15. https://doi.org/10.2174/13892037113149990057.
25. Evans BN, Rosenblatt MI, Mnayer LO, Oliver KR, Dickerson IM. CGRP-RCP, a novel protein required for signal transduction at calcitonin gene-related peptide and adrenomedullin receptors. *J Biol Chem*. 2000;**275**:31438–43. https://doi.org/10.1074/jbc.M005604200.
26. Prado MA, Evans-Bain B, Oliver KR, Dickerson IM. The role of the CGRP-receptor component protein (RCP) in adrenomedullin receptor signal transduction. *Peptides*. 2001;**22**:1773–81. https://doi.org/10.1016/S0196-9781(01)00517-4.
27. McLatchie LM, Fraser NJ, Main MJ, Wise A, Brown J, Thompson N, *et al.* RAMPs regulate the transport and ligand specificity of the calcitonin-receptor-like receptor. *Nature*. 1998;**393**:333–9. https://doi.org/10.1038/30666.
28. Qi T, Hay DL. Structure-function relationships of the N-terminus of receptor activity-modifying proteins. *Br J Pharmacol*. 2010;**159**:1059–68. https://doi.org/10.1111/j.1476-5381.2009.00541.x.
29. Laschinger M, Wang Y, Holzmann G, Wang B, Stöß C, Lu M, *et al.* The CGRP receptor component RAMP1 links sensory innervation with YAP activity in the regenerating liver. *FASEB journal : official publication of the Federation of American Societies for Experimental Biology*. 2020;**34**:8125–38. https://doi.org/10.1096/fj.201903200R.
30. Zhao Z, Fu X, Zhang G, Li Y, Wu M, Tan Y. The influence of RAMP1 overexpression on CGRP-induced osteogenic differentiation in MG-63 cells in vitro: an experimental study. *J Cell Biochem*. 2013;**114**:314–22. https://doi.org/10.1002/jcb.24375.
31. Hay DL, Poyner DR, Sexton PM. GPCR modulation by RAMPs. *Pharmacol Ther*. 2006;**109**:173–97. https://doi.org/10.1016/j.pharmthera.2005.06.015.
32. Udawela M, Hay DL, Sexton PM. The receptor activity modifying protein family of G protein coupled receptor accessory proteins. *Semin Cell Dev Biol*. 2004;**15**:299–308. https://doi.org/10.1016/j.semcdb.2003.12.019.
33. Klein KR, Matson BC, Caron KM. The expanding repertoire of receptor activity modifying protein (RAMP) function. *Crit Rev Biochem Mol Biol*. 2016;**51**:65–71. https://doi.org/10.3109/10409238.2015.1128875.
34. Kurashige C, Hosono K, Matsuda H, Tsujikawa K, Okamoto H, Majima M. Roles of receptor activity-modifying protein 1 in angiogenesis and lymphangiogenesis during skin wound healing in mice. *FASEB journal : official publication of the Federation of American Societies for Experimental Biology*. 2014;**28**:1237–47. https://doi.org/10.1096/fj.13-238998.
35. Yin S, Song R, Ma J, Liu C, Wu Z, Cao G, *et al.* Receptor activity-modifying protein 1 regulates mouse skin fibroblast proliferation via the Gαi3-PKA-CREB-YAP axis. *Cell Commun Signal*. 2022;**20**:52. https://doi.org/10.1186/s12964-022-00852-0.
36. Zhang M, Cao Y, Li X, Hu L, Taieb SK, Zhu X, *et al.* Cd271 mediates proliferation and differentiation of epidermal stem cells to support cutaneous burn wound healing. *Cell Tissue Res*. 2018;**371**:273–82. https://doi.org/10.1007/s00441-017-2723-8.
37. Zhang M, Zhang Y, Ding J, Li X, Zang C, Yin S, *et al.* The role of TrkA in the promoting wounding-healing effect of CD271 on epidermal stem cells. *Arch Dermatol Res*. 2018;**310**:737–50. https://doi.org/10.1007/s00403-018-1863-3.
38. Zhang M, Zhang R, Li X, Cao Y, Huang K, Ding J, *et al.* CD271 promotes STZ-induced diabetic wound healing and regulates epidermal stem cell survival in the presence of the pTrkA receptor. *Cell Tissue Res*. 2020;**379**:181–93. https://doi.org/10.1007/s00441-019-03125-4.
39. Hasan W, Zhang R, Liu M, Warn JD, Smith PG. Coordinate expression of NGF and alpha-smooth muscle actin mRNA and protein in cutaneous wound tissue of developing and adult rats. *Cell Tissue Res*. 2000;**300**:97–109.
40. Shinde AV, Humeres C, Frangogiannis NG. The role of α-smooth muscle actin in fibroblast-mediated matrix contraction and remodeling. *Biochim Biophys Acta Mol basis Dis*. 2017;**1863**:298–309. https://doi.org/10.1016/j.bbadis.2016.11.006.
41. Chin MT, Pellacani A, Wang H, Lin SS, Jain MK, Perrella MA, *et al.* Enhancement of serum-response factor-dependent transcription and DNA binding by the architectural transcription factor HMG-I(Y). *J Biol Chem*. 1998;**273**:9755–60. https://doi.org/10.1074/jbc.273.16.9755.
42. Hay DL, Pioszak AA. Receptor activity-modifying proteins (RAMPs): new insights and roles. *Annu Rev Pharmacol Toxicol*. 2016;**56**:469–87. https://doi.org/10.1146/annurev-pharmtox-010715-103120.
43. Routledge SJ, Ladds G, Poyner DR. The effects of RAMPs upon cell signalling. *Mol Cell Endocrinol*. 2017;**449**:12–20. https://doi.org/10.1016/j.mce.2017.03.033.
44. Penn JW, Grobbelaar AO, Rolfe KJ. The role of the TGF-β family in wound healing, burns and scarring: a review. *Int J Burns Trauma*. 2012;**2**:18–28.
45. Gabbiani G. The myofibroblast in wound healing and fibrocontractive diseases. *J Pathol*. 2003;**200**:500–3. https://doi.org/10.1002/path.1427.
46. Kawamoto M, Matsunami T, Ertl RF, Fukuda Y, Ogawa M, Spurzem JR, *et al.* Selective migration of alpha-smooth muscle actin-positive myofibroblasts toward fibronectin in the Boyden's blindwell chamber. *Clin Sci (Lond)*. 1997;**93**:355–62. https://doi.org/10.1042/cs0930355.
47. Li Y, Li C, Liu Q, Wang L, Bao AX, Jung JP, *et al.* Loss of Acta2 in cardiac fibroblasts does not prevent the myofibroblast differentiation or affect the cardiac repair after myocardial infarction.

J Mol Cell Cardiol. 2022;**171**:117–32. https://doi.org/10.1016/j.yjmcc.2022.08.003.
48. Burr SD, Harmon MB Jr, JAS. The impact of diabetic conditions and AGE/RAGE Signaling on cardiac fibroblast migration. *Front Cell Dev Biol*. 2020;**8**:112. https://doi.org/10.3389/fcell.2020.00112.
49. Rønnov-Jessen L, Petersen OW. A function for filamentous alpha-smooth muscle actin: retardation of motility in fibroblasts. *J Cell Biol*. 1996;**134**:67–80. https://doi.org/10.1083/jcb.134.1.67.
50. Liu Z, Chang AN, Grinnell F, Trybus KM, Milewicz DM, Stull JT, *et al*. Vascular disease-causing mutation, smooth muscle α-actin R258C, dominantly suppresses functions of α-actin in human patient fibroblasts. *Proc Natl Acad Sci USA*. 2017;**114**:E5569–78. https://doi.org/10.1073/pnas.1703506114.
51. Madlener M. Differential expression of matrix metalloproteinases and their physiological inhibitors in acute murine skin wounds. *Arch Dermatol Res*. 1998;**290**:S24–9. https://doi.org/10.1007/PL00007450.
52. Soo C, Shaw WW, Zhang X, Longaker MT, Howard EW, Ting K. Differential expression of matrix metalloproteinases and their tissue-derived inhibitors in cutaneous wound repair. *Plast Reconstr Surg*. 2000;**105**:638–47. https://doi.org/10.1097/00006534-200002000-00024.
53. Moretti L, Stalfort J, Barker TH, Abebayehu D. The interplay of fibroblasts, the extracellular matrix, and inflammation in scar formation. *J Biol Chem*. 2022;**298**:101530. https://doi.org/10.1016/j.jbc.2021.101530.
54. Johnson KR, Lehn DA, Reeves R. Alternative processing of mRNAs encoding mammalian chromosomal high-mobility-group proteins HMG-I and HMG-Y. *Mol Cell Biol*. 1989;**9**:2114–23.
55. Parisi S, Piscitelli S, Passaro F, Russo T. HMGA proteins in Stemness and differentiation of embryonic and adult stem cells. *Int J Mol Sci*. 2020;**21**:362. https://doi.org/10.3390/ijms21010362.
56. Shah SN, Kerr C, Cope L, Zambidis E, Liu C, Hillion J, *et al*. HMGA1 reprograms somatic cells into pluripotent stem cells by inducing stem cell transcriptional networks. *PLoS One*. 2012;**7**:e48533. https://doi.org/10.1371/journal.pone.0048533.
57. Zhao C, Li Y, Zhang W, Zhao D, Ma L, Ma P, *et al*. IL-17 induces NSCLC A549 cell proliferation via the upregulation of HMGA1, resulting in an increased cyclin D1 expression. *Int J Oncol*. 2018;**52**:1579–92. https://doi.org/10.3892/ijo.2018.4307.
58. Zhang S, Lei R, Wu J, Shan J, Hu Z, Chen L, *et al*. Role of high mobility group A1 and body mass index in the prognosis of patients with breast cancer. *Oncol Lett*. 2017;**14**:5719–26. https://doi.org/10.3892/ol.2017.6963.
59. Fu F, Wang T, Wu Z, Feng Y, Wang W, Zhou S, *et al*. HMGA1 exacerbates tumor growth through regulating the cell cycle and accelerates migration/invasion via targeting miR-221/222 in cervical cancer. *Cell Death Dis*. 2018;**9**:594. https://doi.org/10.1038/s41419-018-0683-x.
60. Egawa N, Hamanaka G, Chung KK, Ishikawa H, Shindo A, Maki T, *et al*. High mobility group A1 regulates transcription levels of oligodendrocyte marker genes in cultured oligodendrocyte precursor cells. *Int J Mol Sci*. 2022;**23**:2236. https://doi.org/10.3390/ijms23042236.
61. Xie Q, Yao Q, Hu T, Cai Z, Zhao J, Yuan Y, *et al*. High-mobility group A1 promotes cardiac fibrosis by upregulating FOXO1 in fibroblasts. *Front Cell Dev Biol*. 2021;**9**:666422. https://doi.org/10.3389/fcell.2021.666422.
62. Strauch AR, Hariharan S. Dynamic interplay of smooth muscle α-actin gene-regulatory proteins reflects the biological complexity of Myofibroblast differentiation. *Biology (Basel)*. 2013;**2**:555–86. https://doi.org/10.3390/biology2020555.
63. Hopper RK, Moonen JR, Diebold I, Cao A, Rhodes CJ, Tojais NF, *et al*. In pulmonary arterial hypertension, reduced BMPR2 promotes endothelial-to-mesenchymal transition via HMGA1 and its target slug. *Circulation*. 2016;**133**:1783–94. https://doi.org/10.1161/CIRCULATIONAHA.115.020617.
64. Tang PM, Zhang YY, Xiao J, Tang PC, Chung JY, Li J, *et al*. Neural transcription factor Pou4f1 promotes renal fibrosis via macrophage-myofibroblast transition. *Proc Natl Acad Sci USA*. 2020;**117**:20741–52. https://doi.org/10.1073/pnas.1917663117.

Burns & Trauma, 2025, 13, tkae068
https://doi.org/10.1093/burnst/tkae068
Research Article